



Peculiarity of magnetization relaxation in finite size superconductors

L.S. Uspenskaya ^{a,*}, K.S. Korolev ^a, P.N. Yarykin ^b

^a *Institute of Solid State Physics, Russian Academy of Sciences, Chernogolovka, Moscow District 142432, Russia*

^b *Department of Mechanics and Mathematics, Moscow State University, Russia*

Received 1 April 2005; received in revised form 14 April 2005; accepted 14 April 2005

Abstract

Our experimental data on relaxation of partially penetrated remnant flux in YBCO thin samples shows different rate of relaxation at the outer front of the magnetic flux and at the inner front, whereas in thick samples this rate is approximately the same. To clarify the origin of this difference a computer simulation of the process was undertaken. Both experimental data and simulation suggest that shape of the sample is the key factor.

Different relaxation of flux at outer and inner front leads to important consequence: dependence of relaxation of trapped flux upon its configuration, in particular, slow relaxation of alternate flux compared with relaxation of unidirectional flux.

© 2005 Elsevier B.V. All rights reserved.

PACS: 74.72.Hs; 74.60.Ge; 74.60.Jg; 74.25.Ha

Keywords: HTSC; Critical current; Magnetization; Relaxation; Creep; Magneto-optics

1. Introduction

The question, what kind of relaxation of magnetization might be observed in superconductors of finite size is still under discussion [1–10], though it was considered widely since the discovery of type

II superconductivity. This process is interesting because it provides knowledge about behavior of vortices, their interaction, and thermoactivated motion. It is also very important for bulk superconductor applications in levitation devices, motors, generators, and bearings. Moreover, in finite plates magnetization relaxation is of particular importance for bulk superconductor applications, where plate-like superconducting elements are not in full critical state. For optimal construction of such

* Corresponding author. Tel.: +7 96 5249498; fax: +7 96 5249701.

E-mail address: uspenska@issp.ac.ru (L.S. Uspenskaya).

devices it is important to know both time dependence, which is mostly studied, and magnetic flux redistribution, which occurs with time. Here magnetization relaxation in YBCO plates is studied by magneto-optical technique, MO, that allows us to determine mean current, magnetization relaxation, and spatial changes of magnetization distribution.

2. Experimental

The experiments are performed with optimally doped YBCO single crystals, and melt-textured single domain YBCO, $T_c = 93$ K, using magneto-optical technique. All samples have rectangular shape, and the main plane coincides with crystallographic ab -plane. Linear sizes of the samples are varied from 0.2 to 2 mm, and thickness from 0.01 to 2 mm.

Relaxation of magnetic flux, which penetrates into the sample under external magnetic field, as well as relaxation of trapped magnetic flux after zero field cooling (ZFC), and after cooling under some external magnetic field (FC) in wide temperature range is studied.

Well known, magneto-optical technique (MO) allows one to visualize distribution of component of magnetic induction B_z perpendicular to the sample's plane by means of thin optically active indicator film placed directly on the surface of the studied sample.

Observations of distribution of B_z are performed with polarized-light microscope in reflected light. The indicator locally rotates polarization of incident light by some angle ϕ , which is proportional to local $B_z(x, y)$. $\phi \sim \tan \phi \sim B_z/B_a$ where B_a is the saturation field of indicator, which is higher than 3000 Oe in our case. Rotation of polarization causes the variation of brightness of pattern, which depends upon ϕ and the angle between polarizer and analyzer prisms. Maximum polarization rotation, ϕ_{\max} is determined by indicator chemistry and thickness, here ϕ_{\max} is about 10° . In our experiments polarizer and analyzer prisms are uncrossed for the angle $\sim \phi_{\max}$, which allows us to recover real flux density from obtained patterns through comparison of local brightness

of initial images with the brightness of the set of calibration images taken at different fields at temperature T , which is slightly higher than T_c . This provides us with reliable information about magnetization distribution.

However, in theories one often speaks about current relaxation, not about magnetization relaxation. Finding the exact current distribution from $B_z(x, y)$ distribution is difficult because common formula $j \sim dB/dx$ is not valid for finite size sample and correct extraction of current distribution from $B_z(x, y)$, obtained experimentally, is impossible [11].

This ill-conditioned problem could be solved directly only for a sample with finite size if one supposes that current only depends upon two coordinates, $\vec{j} = \vec{j}(x, y)$, and does not change along z -axis, which coincides with field direction, $\vec{j} \neq \vec{j}(z)$. This assumption is true only in the case when the whole sample is in critical state. Nevertheless, we can find one among others possible $\vec{j}(x, y)$ distributions, which produces this $B_z(x, y)$ following some "hand-made" reasonable suggestions about current flow into the sample, like it was done in [12]. We use a few suggestions: magnetic field penetrates into the sample from sides, which are parallel to the field, penetration volume is restricted inside the sample by inscribed ellipsoid, and initial current with constant value flows everywhere in the volume where the field has penetrated (see insert in Fig. 1). All three points are in agreement with E.H. Brandt calculations of flux penetration in superconductor of finite size.

So we have a satisfactory agreement between experimental profiles of magnetic induction and its derivatives, $B_z(x, y)$, $\partial B_z(x, y)/\partial x$, $\partial B_z(x, y)/\partial y$ with appropriate simulation curves everywhere but the very sample interior, where inscribed ellipsoid approaches very close to the sample surface. Dependencies $B_z(x)$, $dB_z(x)/dx$ calculated along the middle cross section of the sample for $y = \text{const}$, for particular sample with ratio of height and width, $k = 7/200$, with field penetration depth $d = 99\%$, 80% , 50% , 20% of full penetration, are shown in Fig. 1. One can see that field penetration depth is easily determined from $dB_z(x)/dx$ despite of complicated shape of front of penetrated field. Moreover, the main part of $dB_z(x)/dx$ does not

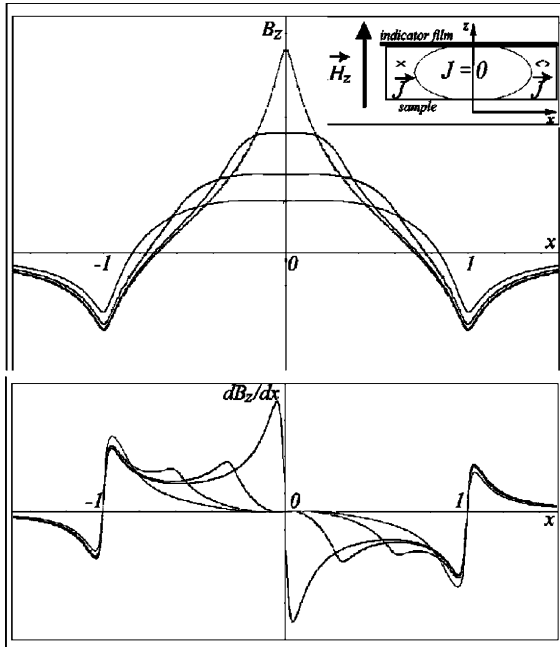


Fig. 1. Calculated profiles of trapped flux distribution after FC and correspondent flux gradient for the sample with aspect ratio $k \sim 30$ (profiles are equivalent for penetration profiles after ZFC).

depend upon this shape. So it is a way to determine penetration depth from experimental curves $B_z(x)$. Good agreement between calculated $dB_z(x)/dx$ and experimentally measured $dB_z(x)/dx$ confirms that this is the right way to determine a current value, by finding a current that gives a theoretical curve coinciding with experimental one. The same procedure as described above is used for simulation of trapped flux distribution, Fig. 2. Note, profiles $B_z(x)$ are not symmetric relative to the maximum of trapped flux when the current of the same value flow in different directions in inner and outer parts of trapped flux. Analyzing plots of $B_z(x)$ and $dB_z(x)/dx$ we state again, that the most information about penetration and current can be obtained from $dB_z(x)/dx$ and not from $B_z(x)$, which have complicated shape and are very sensitive to the distance between indicator and the sample surface. Therefore derivatives are used for analysis of all experimentally obtained profiles.

The field up to 2700 Oe can be applied perpendicular to the sample crystallographic ab -plane in

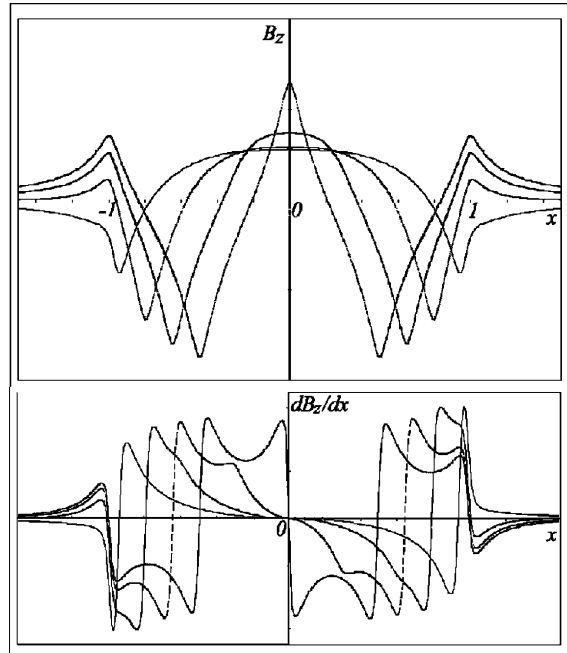


Fig. 2. The same for the remnant flux after partial field penetration.

our experiments. This field was high enough for full penetration into the samples at $T > 24$ K and low enough to be observed by MO. The observation of magnetization relaxation is started from the moment of pulse magnetic field switching off (with rising time $t \sim 1$ ms) and is performed during time interval $t \sim 2000$ s.

3. Experimental results

We studied penetration of magnetic field and relaxation of trapped flux obtained both by cooling in magnetic field and by exposure to external magnetic field after zero field cooling. It is well known that two configurations of trapped flux can be formed depending on the strength of applied magnetic field. For zero field cooling if the magnetic field strength is higher than $2H_p$, where H_p is a field of full penetration, trapped flux is spread over the whole sample with maximum density at the center; if the external magnetic field is lower than $2H_p$, distribution of magnetic induction has two distinct maxima, which are located the

deeper the stronger the field. We found that while conventional relaxation of magnetization takes place for fully penetrated state, there are some peculiarities for partially penetrated state.

At first, we consider relaxation of remnant flux in thin single crystal samples, for which typical

results are presented in Fig. 3. Experimental images of trapped flux before and after relaxation within 2000 s, and their difference are shown in Fig. 3(a); areas with higher values of magnetic induction are brighter. The crystal has twin structure at the top half and it is twin-free elsewhere. This results in more pronounced turbulence [14] at the edges of the sample, where reverse flux relaxes. However, from the pictures it is clear that at the given temperature penetration depth does not vary along the sample, therefore pinning force is the nearly same throughout the crystal.

From difference image it is clear that relaxation takes place all over the crystal, particularly, there is no significant difference between the center and the edges. Initial and final profiles of magnetic induction along the drawn line are presented in Fig. 3(b). Time dependence of whole sample magnetization relaxation along with current decay is depicted in Fig. 3(c); the current is extracted from profiles as it is described in the previous section. One can see simple linear dependence of magnetization and critical current on $\ln(t)$, which is in full agreement with both theoretical predictions and macroscopic measurements [2].

The picture changes drastically, when there are two currents of opposite sign in the sample. It is realized if external field $H_z < 2H_p$ is applied and switched off. Two different relaxations of magnetization are observed in this case. The first relaxation, slow, takes place at the inner flux part, and the second—fast one, at outer flux part, closer to sample edges. It is also important to mention that vortices do not propagate to the sample interior during relaxation. This can be seen on in Fig. 4, where remnant flux distribution, the difference between initial and final distribution, initial and final $B_z(x)$ profiles taken along the drawn line, and time dependence of magnetization and critical current are shown. The different rate of relaxation is evident from experimental images Fig. 4(a), where the bright region in the picture presenting diminution of trapped flux is more narrow than in two other images, and this shows that intensive relaxation doesn't take place in the whole region with magnetic field. In Fig. 4(b,c) one can see that relaxation at outer front obeys the same law as in the previous case, though with slightly different

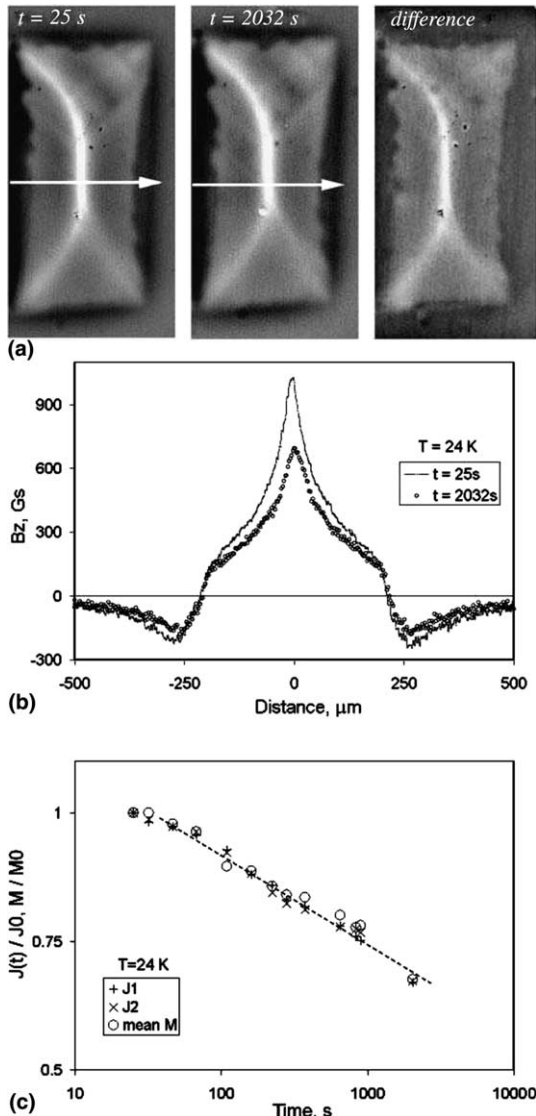


Fig. 3. Relaxation of trapped flux for fully penetrated state; aspect ratio, k , for this sample is 0.02. (a) Remnant magnetic flux distribution after 25 s, after 2032 s and their difference (drawn line shows the direction where $B_z(x)$ were taken), (b) profiles $B_z(x)$ and (c) relaxation of magnetization and current.

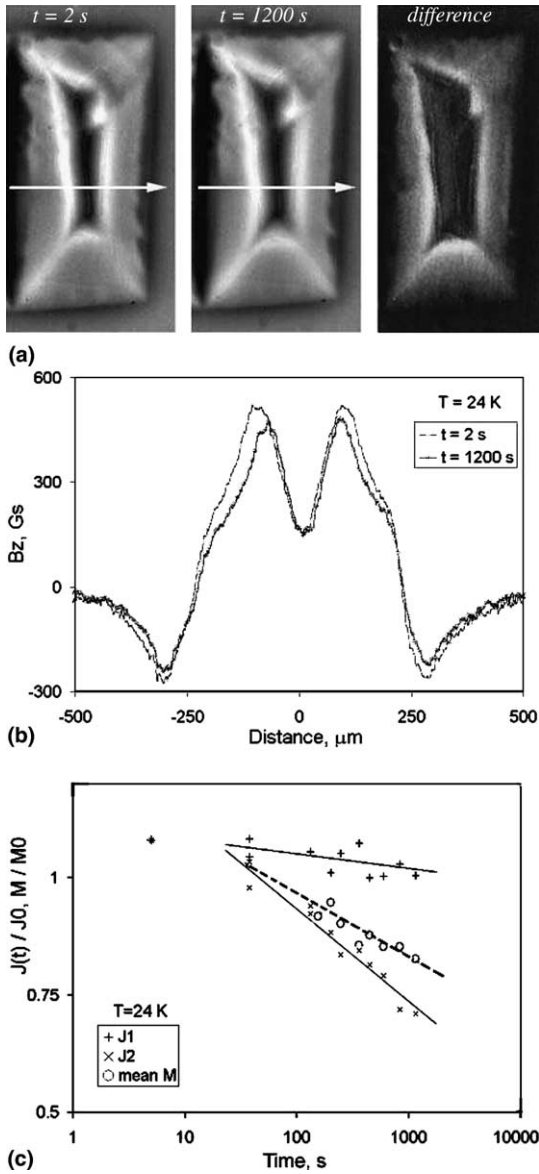


Fig. 4. The same as in Fig. 3 but for partially penetrated state.

$\partial \ln(j)/\partial \ln(t)$, whilst magnetic field and its gradient seem to remain nearly the same at the inner front. Note, that the higher the temperature, the more pronounced discrepancy in difference between slopes of dependencies j/j_0 against $\ln(t)$ for these two relaxation. We want to emphasize that slow relaxation at the middle of the sample and fast relaxation at the edges was observed in all our single crystals, which were thin plates.

Completely different behavior is observed on thicker samples with aspect ratio ~ 1 . Typical results are presented in Fig. 5, where one can see initial and final flux density distribution, their difference and profiles taken along the drawn line. Major peculiarity of relaxation compared to relaxation of magnetic induction in thin samples is similar magnetization relaxation rates at inner and outer fronts of magnetic field. It is also important that flux propagates to the samples interior if penetration depth is smaller, i.e. when applied field is less than H_p . While we emphasize different aspect ratio we have to mention that these experiments were carried out on melt textured samples, because nowadays the composite YBCO are more perfect and more homogeneous than thick single crystals. Note, thin composite crystals as well as thin single crystals show different relaxation rate at outer part of the flux and at the inner part.

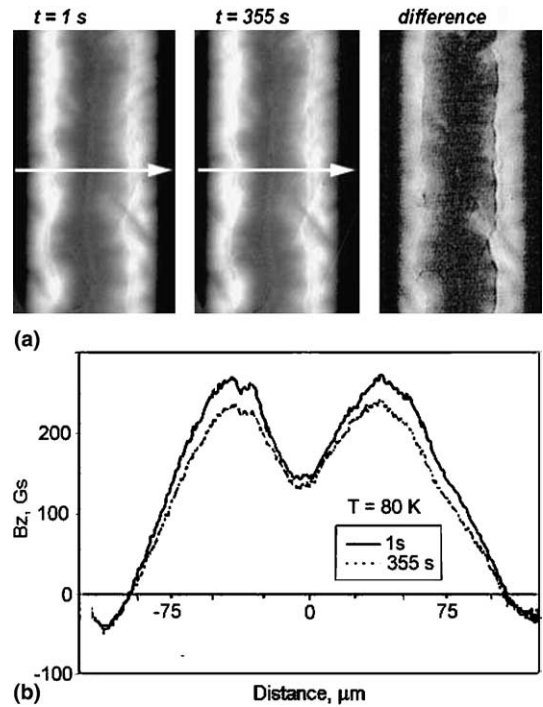


Fig. 5. Relaxation of trapped flux for partially penetrated state; $k = 1$. (a) Remnant magnetic flux distribution after 1 s, after 355 s and their difference (drawn line shows the direction where $B_z(x)$ were taken) and (b) profiles $B_z(x)$.

Significant difference in relaxation rates within thin samples and more uniform relaxation for thicker samples was observed in all our experiments with different penetration depths, which shows irrelevance of relaxation of intermediate part of the sample, that is not in full critical state, see Fig. 1. Moreover, such behavior is observed in wide temperature range from 24 to 80 K, within which relaxation rate changes substantially and critical current varies from 10^6 to 10^3 A/cm². What is more important is that this phenomenon occurs in presence of different mechanisms of pinning, at temperatures below 30 K vortices are pinned mainly on oxygen vacancies while at higher temperatures they are efficiently pinned by planar defects. As this effect is observed despite variety of microscopic changes, the difference in relaxation rates is rather sample governed than material governed. All above suggests that this macroscopic phenomenon may be explained by different aspect ratio and consequently by different geometrical conditions. To clarify this hypothesis theoretical consideration is presented.

4. Simulation of field and current relaxation

We assume superconductor to be parallelepiped and apply field along z -axis perpendicular to the sample's plane. To find time dependence of magnetic field, current, and electric field we use the following equations:

$$\text{rot}(\vec{E}) = -\frac{\partial \vec{B}}{\partial t}, \quad \text{Maxwell equation}; \quad (1)$$

$$\vec{B} = \frac{\mu_0}{4\pi} \int_V \frac{[\vec{j}, \vec{r}]}{r^3} d^3\vec{r}, \quad \text{Bio-Savart law}; \quad (2)$$

$$\vec{E} = \vec{E}(\vec{j}, \vec{B}), \quad \text{Material equation}; \quad (3)$$

which can be solved in terms of magnetic induction by inverting Bio-Savart law (2) and substituting $\vec{j}(\vec{B})$ and $\vec{E}(\vec{j}(\vec{B}), \vec{B})$ into Eq. (1).

A few approaches for material equation exist at the moment, and there is a discussion which one describes superconductor better. Two of them, which are mostly used [15] are:

$$\vec{E} = E_c \frac{\vec{j}}{|\vec{j}|} \left(\frac{j}{j_c} \right)^n, \quad E-j \text{ approach}; \quad (4)$$

$$\vec{E} = B v_c \frac{\vec{j}}{|\vec{j}|} \left(\frac{j}{j_c} \right)^n, \quad \text{Flux creep approach}; \quad (5)$$

where j_c is critical current and E_c , v_c , and n are parameters. In our simulation both approaches give similar results. $E-j$ approach is used here due to convenience.

System of equations (1), (2), (4) can be solved easily, if there is a simple way to invert Bio-Savart law (2). This is possible in two opposite approximations, namely, when the ratio of sample height over width k is either much bigger than unity ($k \gg 1$) or much less ($k \ll 1$). These two cases are considered below.

4.1. Infinite plate case ($k \gg 1$)

At first, we consider approximation of infinite plate, sample is assumed to be infinite along y and z dimensions, thus we only take into account properties of the superconductor as a material. In this case inverse of Bio-Svarat law (2) can be reduced to [5–7,15]:

$$\mu_0 j = -\partial B / \partial x, \quad (6)$$

where j is directed along y axis. This allows to solve system of equations (1), (2), (4) easily. Using this approach, we simulate relaxation of trapped flux for full and partial penetration. Solutions are presented in Fig. 6.

The first plot (Fig. 6a), corresponding to full critical state, shows that magnetic induction decreases with time, preserving almost triangular shape of its profile. This according to Eq. (6) means the current distribution remains the same while current density decays. In the plot for partial penetration (Fig. 6b) one can see that along with decreasing of flux density redistribution of magnetic induction takes place. Whereas at outer fronts critical current diminishes like it was for fully penetrated state.

Both fully and partially penetrated state shows approximately logarithmic law of flux and current decay (Fig. 7) with deviations from this law at the initial and final stages of relaxation. We did

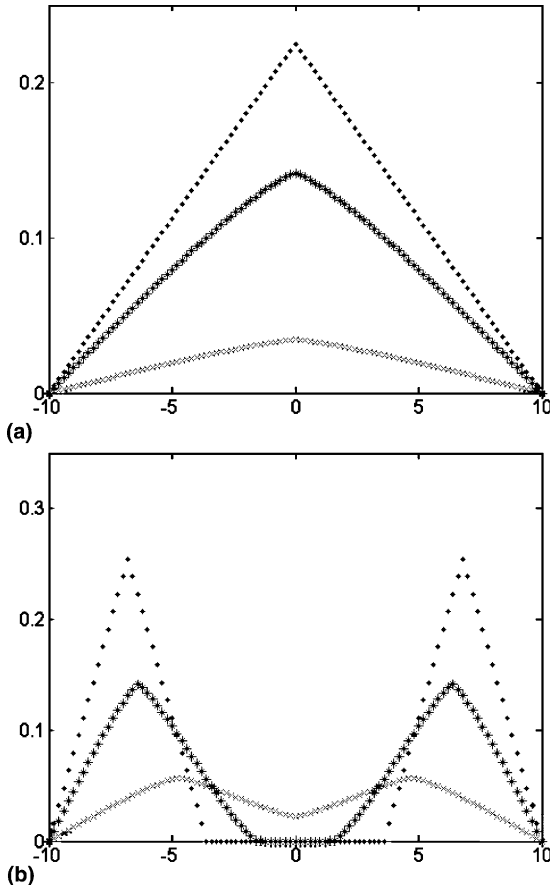


Fig. 6. Modification of magnetic induction distribution calculated for infinite plate. (a) Fully penetrated state and (b) partially penetrated state.

observe such behavior in measurements with thick melt-textured samples as well as with thin single crystal samples.

Note, in our simulation total magnetization of the sample decreases slower for partly penetrated state.

Main feature of the simulated process presented above is that relaxation rate at outer and inner fronts is nearly the same for partly penetrated state and flux enters sample's interior. These two facts completely disagree with our experimental data for thin samples. Because of this we consider a strip case ($k \ll 1$), which geometrically is much closer to our experiment than the first one, because ($k \approx 0.04$ for our sample).

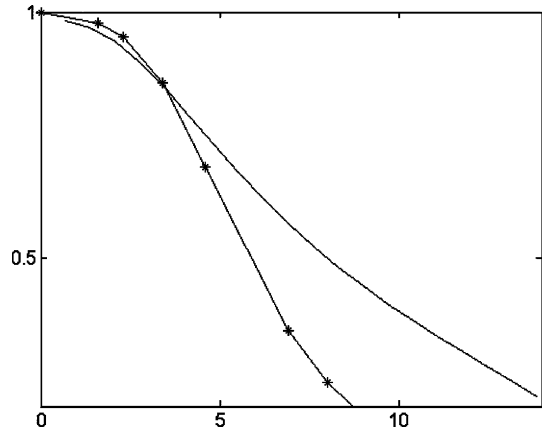


Fig. 7. Mean magnetization relaxation calculated for fully penetrated state (curve with dots) and partially penetrated state (solid line) for infinite plate.

4.2. Strip case ($k \ll 1$)

We assume sample to be of zero thickness along z dimension and infinite length along y dimension. Magnetic field is directed perpendicular to the surface of superconductor. In this situation inverse Bio–Savart law can be written now as [15]:

$$j(x) = \frac{2}{\pi d \mu_0} \int_{-w}^w \frac{B(x') - H_{\text{ext}}}{x - x'} \sqrt{\frac{w^2 - x'^2}{w^2 - x^2}} dx', \quad (7)$$

where $2w$ is the width of the superconductor. Our simulation made in this approach shows nearly the same logarithmic decay of total current and flux for partially and fully penetrated state, but relaxation of distribution of current and magnetic field is significantly different.

Results for fully penetrated state are presented in Fig. 8. One can see modification of magnetic field distribution during relaxation without considerable spacial changes like in previous case. It is important to mention that profiles don't tend to have triangular shape now. Moreover, the curvature of $B(x)$ is the opposite compared to infinite plate case, which is always observed for thin plates. For partially penetrated state, however, very special behavior is found, see Fig. 9. First of all, one can see faster rate of relaxation at outer front than at inner front, like it was observed in our experiments. In addition, magnetic field doesn't enter

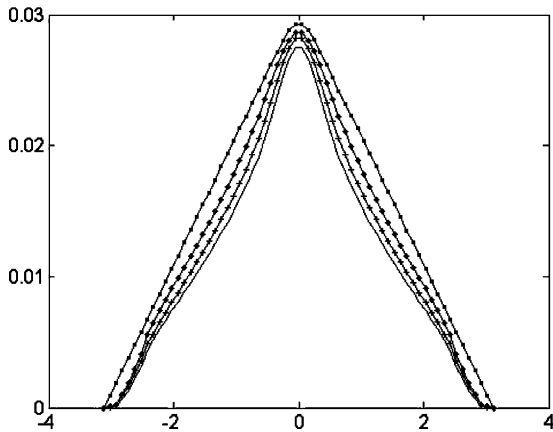


Fig. 8. Modification of calculated magnetic induction distribution for fully penetrated state in thin strip approximation.

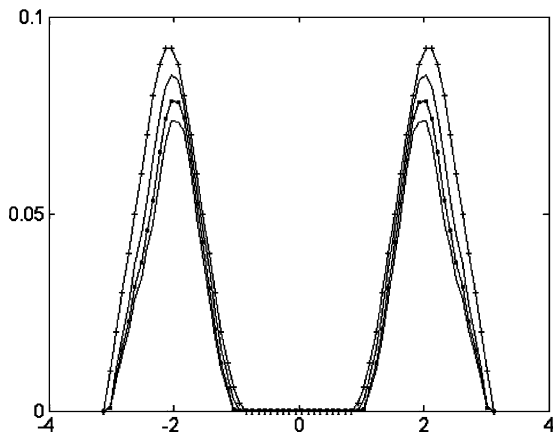


Fig. 9. Modification of calculated magnetic induction distribution for partially penetrated state in thin strip approximation.

inner part of the sample during relaxation, which is also confirmed by our measurements.

Consideration of a thin strip gives us some understanding about the causes for the significant difference between relaxation of partly penetrated state in an infinite plate and in a strip. Due to very non-local relationship between current and magnetic field (7), i.e. when magnetic field is determined by current distribution in the whole sample rather than by current at a given point, it may happen that current is substantially different in the areas, where magnetic field is the same. And even a small difference results in significantly different

relaxation rate due to non-linear relationship between current and electric field (4), which determines the relaxation according to Eq. (1).

5. Discussion

Effect of different relaxation rate at inner and outer front of trapped magnetic flux is observed in thin superconductor plates. Such behavior was observed in wide range of temperature (20–80 K), i.e. for different mechanisms of pinning. Our simulation shows that this behavior can be explained even without consideration of creep nature by taking into account only geometrical factor, namely the ratio, k , of height over width. When $k \gtrsim 1$ or $k \gg 1$ (6) is valid, which states that current $\vec{j}(\vec{r})$ at a given point \vec{r}_0 is determined by magnetic induction $\vec{B}(\vec{r})$ in close proximity of \vec{r}_0 . When $k \ll 1$ any local dependence is valid no more. This simple fact leads to far reaching consequences. Firstly, this can explain why small radio frequency noise can reduce relaxation [10,13] and flux creep in different types of superconductor devices. Secondly, it is very important to take into account effect in question for correct interpretation of measurements of the whole sample magnetization, because they may give some average of two completely different relaxations. Finally, understanding of how relaxation depends on geometry of the sample, particularly how distribution of field and current influence each other can play important role in understanding the way twistors are formed.

Acknowledgement

The authors acknowledge E.H. Brandt, L.M. Fisher, M.V. Indenbom, G.P. Mikitik, A.L. Rakhmanov, V.V. Ryazanov, and V.A. Yampolskii for useful discussions, G.A. Emelchenko, A.B. Kulakov, I.G. Naumentko, G. Krabbes for supplying samples and Alexander von Humboldt Foundation for providing us with part of optical equipment.

This work is supported by INTAS (grant 01–2282), RFBR (grant 05–02–17166).

References

- [1] Y. Yeshurun, A.P. Malozemoff, *Phys. Rev. Lett.* 60 (1988) 2202.
- [2] Y. Yeshurun, A.P. Malozemoff, A. Shaulov, *Rev. Mod. Phys.* 68 (1996) 911.
- [3] G. Blatter, M.V. Feigelman, A.I. Larkin, V.M. Vinokur, *Rev. Mod. Phys.* 66 (1994) 1125.
- [4] A. Gurevich, H. Kupfer, *Phys. Rev. B* 48 (1993) 6477.
- [5] E.H. Brandt, *Phys. Rev. Lett.* 76 (1996) 4030.
- [6] E.H. Brandt, *Rep. Prog. Phys.* 58 (1995) 1465.
- [7] I.M. Babich, G.P. Mikitik, E.H. Brandt, *Phys. Rev. B* 68 (2003) 052509.
- [8] G.P. Mikitik, E.H. Brandt, M. Indenbom, *Phys. Rev. B* 70 (2004) 014520.
- [9] D.V. Shantsev, Y.M. Galperin, T.H. Johansen, *Phys. Rev. B* 65 (2002) 184512.
- [10] L.S. Uspenskaya, *Superconductivity: research and development*, 12 (2004).
- [11] M. Eisterer, *Supercond. Sci. Technol.* 18 (2005) S58–S62.
- [12] L. Uspenskaya, V. Vlasko-Vlasov, V. Nikitenko, T. Johanson, *Phys. Rev. B* 56 (1997) 11979–11988.
- [13] A. Kalinov et al., Thesis of “First conference on fundamental problems of superconductivity”, Moscow 2004, p. 123.
- [14] L.S. Uspenskaya, I.G. Naumenko, A.A. Zhoklov, *Physica C* 402 (2004) 188–195.
- [15] D.V. Shantsev, A.V. Bobyl1, Y.M. Galperin, and T.H. Johansen, arXiv:cond-mat/0003396; D.V. Shantsev, A.V. Bobyl1, Y.M. Galperin, T.H. Johansen, *Physica C* 341 (2000) 1145.